Materials Transactions, Vol. 48, No. 9 (2007) pp. 2506 to 2512

Fabrication and Thermal Properties of Carbon Nanotube/Nickel Composite by Spark Plasma Sintering Method*

Shunsuke Yamanaka[1], Ryohei Gonda[1], Akira Kawasaki[1], Hiroki Sakamoto[2], Yutaka Mekuchi[2], Masaki Kuno[2] and Takayuki Tsukada[3]

[1]*Department of Materials Processing Engineering, Graduate School of Engineering, Tohoku University, Sendai 980-8579, Japan*
[2]*Material Research Laboratory, Nissan Motor Co., Ltd., Yokosuka 237-0061, Japan*
[3]*Nano carbon technologies Inc., Tokyo 194-0014, Japan*

Multiwall carbon nanotube (MWNT) materials are attractive because they possess excellent thermal conductivity and mechanical properties. However, few reports exist that focus on improving the thermal conductivity of MWNT by combining it with a metal matrix. Thus to improve the thermal conductivity, a nickel-matrix composite with MWNT was prepared by slurry mixing process using ethanol as a solvent. Using spark plasma sintering (SPS), MWNT/Nickel nanocomposites were fabricated and the fabrication conditions were investigated. The sintered relative densities of the composites containing up to 5 vol% of MWNT were above 99%. The thermal and electrical behaviors of the MWNT/Nickel composites were determined using the laser flash and van der Pauw methods, respectively, and were found to be anisotropic. The thermal conductivity was found to increase by 10% for the composition with 3 vol% MWNT. [doi:10.2320/matertrans.MRA2007084]

(Received April 12, 2007; Accepted June 19, 2007; Published August 1, 2007)

Keywords: *carbon nanotube, metal matrix composite, thermal conductivity, electrical conductivity, spark plasma sintering, nanocomposite*

1. Introduction

In the field of material science, there is a significant advantage when materials with specific properties may be designed for specific purposes. Such properties depend on the material content ratio and geometry. However, it is not an easy task to achieve the targeted characteristics for a composite due to the difficulties arising from interfaces and dispersion.

It has been reported that carbon nanotube (CNT) materials have a low density with excellent mechanical strength and the possibility of exhibiting characteristics superior to those of diamond, in terms of thermal conductivity, is anticipated.[1)] Researches up to now have mostly focused on composites comprising CNT and ceramics or polymers. However, few studies have been carried out on composites of CNTs with metals. As a nanostructured CNT is cohesive due to van der Waals forces, it is difficult to homogeneously distribute it in a matrix. Since CNTs have few defects on their surface, it is difficult to achieve wetability and adhesion through the conventional fabrication process; thus, a new method is necessary. It is thought that the performance of a metallic material can be greatly improved by adding a small amount of CNT, that is, if the metallic radical in the CNT composite material can be homogeneously distributed.

The thermal conductivities of CNT composite materials that have been reported thus far are shown in Table 1.[2–5)] Thus, there is no established method to effectively demonstrate the improvement of thermal conductivity by CNT compounds.

Generally, graphite is known as a semiconductor with zero band gap that contributes extremely few electrons, which affects the thermal conductivity from an expected high lattice vibration. Since CNTs are also a type of graphite, a similar phenomenon is expected. In the present study, nickel is selected as the matrix and the effect of CNT composite on the thermal characteristic is investigated and the combination of nickel and CNT is also examined. The reason for this selection is that carbide is easily available and its sinterability is good. Fine Ni powders are utilized to achieve a homogenous dispersion and stability. The improvement in the thermal characteristics is investigated by adopting the colloidal mixing method and spark plasma sintering (SPS) method as the fabricating process for the Ni/CNT composites. The colloidal suspension method uniformly distributes and mixes the multiwalled CNTs (MWNTs) in the metal matrix. Multiwalled CNT is utilized due to its lower cost and smaller specific surface area as compared to singlewalled CNTs.

Table 1 Thermal conductivities of some composites.

Matrix	Matrix λ/Wm^{-1}K^{-1}	CNT content /vol%	Composite λ/Wm^{-1}K^{-1}	$\Delta\lambda$	Reference
epoxy resin	0.15	0.6	0.45	0.30	2
epoxy	0.2	0.1	0.33	0.11	3
epoxy	0.12	1	0.16	0.04	4
Alumina	27.3	10	11.4	−15.9	5
Aiumina	27.3	15	7.3	−20.0	5
Nickel	69.3	1	70.3	1.00	this paper
Nickel	69.3	3	75.8	6.50	this paper

The influence of the fabrication method on the composite structure, particularly the dispersion of CNT is investigated. Moreover, the influence of combining CNT with metal on the thermal, electrical, and physical properties is also considered.

2. Experimental

The powder raw material is a multiwall CNT (Nano carbon

*This Paper was Originally Published in Japanese in J. Japan Inst. Metals **70** (2006) 721–728.

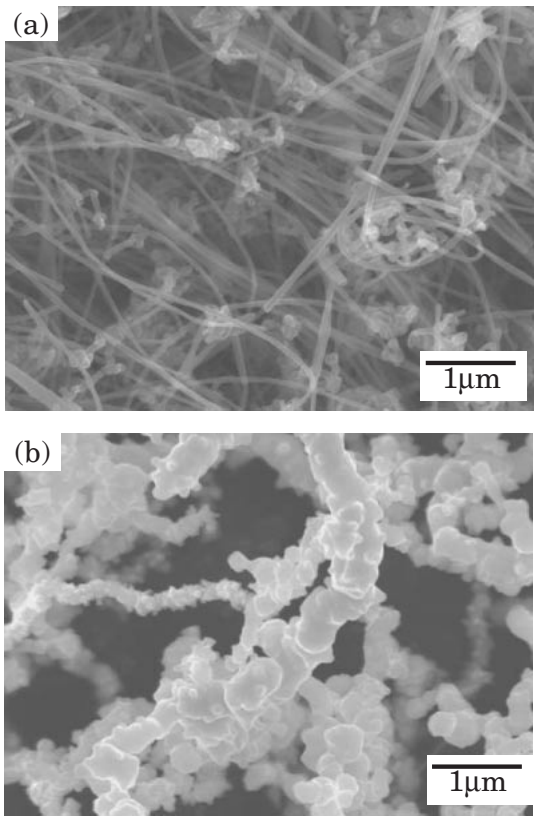

Fig. 1 SEM photographs of raw powders; (a) CNT (b) nickel.

technologies Inc.; #040618) with an average particle diameter of approximately 20–70 nm. Figure 1(a) shows an SEM photograph of MWNT. The size distribution is comparatively small as compared to the diameter, which is approximately 50 nm for any CNT. As for the shape, the bent CNTs are intertwined, as seen in the photograph. For the raw Ni powder (High purity chemical Ltd.), the average particle size is approximately 1 μm. Figure 1(b) shows an SEM photograph of the Ni powder. The particles are confirmed to be approximately 300 nm and are connected not by van der Waals forces but through the process of manufacturing (electrolysis method).

Figure 2 shows the process flow chart for the CNT composite fabrication procedure. To produce the Ni/CNT precursors, the mixture is stirred with an ultrasonic homogenizer and a scroller is used as a means to obtain a homogenous mixture. This precursor is dried for 24 h using a porous Al_2O_3 board. An SPS machine (Sumitomo Coal Mining Co., Ltd.; SPS-511S) is subsequently used for the sintering process. The sintering temperature for Ni is 1273–1573 K[6] and proceeds at a low rate of sintering while being energized by the SPS. Subsequently, the sintering conditions are set at a heating and cooling rate of 50 K/min with a holding time of 1 min at the soaking temperature. The composite is sintered within the sintering temperature range of 673–1073 K and the conditions of fabrication are investigated. The sintering pressure is 50 MPa in vacuum (< 5 Pa) using a die made of carbon with an internal diameter of 15 mm. The thermal diffusivity of the composite after sintereing was measured using a laser flash device (NETZSCH: LFA-427). The thermal conductivity was

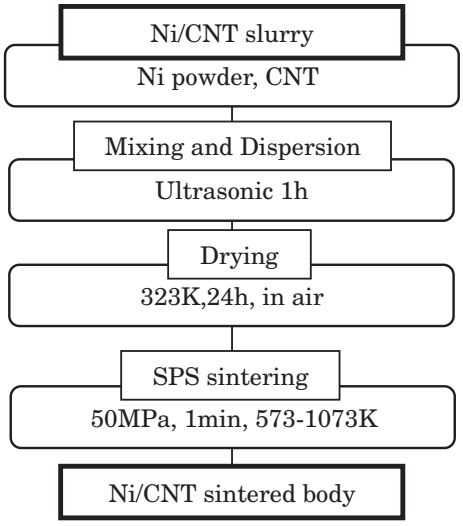

Fig. 2 Experimental procedure for fabrication of Ni/CNT composite.

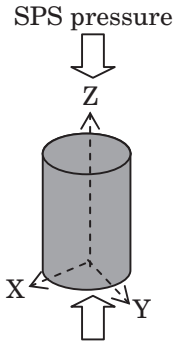

Fig. 3 Schematic diagram of Ni/CNT composite direction of X, Y and Z under SPS in this paper.

calculated using the expression from measurements of thermal diffusivity.

$$\lambda = \alpha C_p D \quad (1)$$

where C_p is the specific heat (kJ/kgK) and D is the density (Mg/m^3) obtained at room temperature (298 K). The specific heat of CNT was assumed to be 0.690 (kJ/kgK) (specific heat of the carbon black)[7] and the specific heat of Ni is 0.439 (kJ/kgK)[7] as calculated from the rule of mixtures.

The electrical conductivity of the composite was measured by the van der Pauw method. The measured current flow was 100 mA, obtained at room temperature (298 K). Figure 3 shows a schematic diagram of the Ni/CNT composite in the X, Y, and Z directions under SPS.

3. Results and Discussion

An SEM photograph of the dried Ni/5 vol% CNT precursor is shown in Fig. 4(a) and Fig. 4(b). The sample with insufficient ethanol is observed in the aggregate form in (a), while the uniformly distributed CNTs in the same sample with the appropriate amount of ethanol are shown in (b). Such observations are thought to depend on the form-factor effect and the hetero-aggregation action. Recohesion by van der

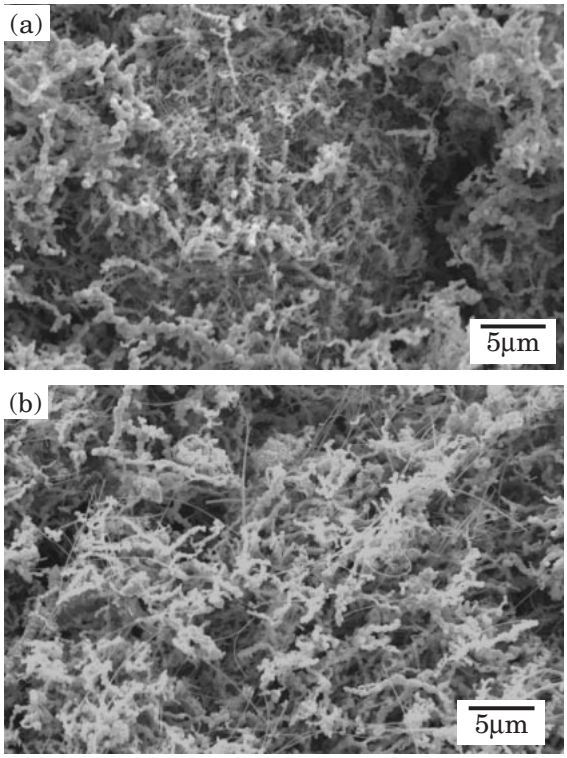

Fig. 4 SEM micrographs of dried Ni/5 vol%CNT powders with (a) 50 ml solvent (b) 100 ml solvent.

Waals forces is controlled by the form factor, which affects the CNTs distributed in between the Ni particles through ultrasonification. On the other hand, hetero-aggregation is generated by the charge difference between the Ni particle and CNT in the solvent.

It is difficult to fabricate composites by nonpressure sintering because CNTs may obstruct the union of particles with Ni and not sinter into a composite. Moreover, the charge and disappearance of the CNT structure has been reported due to the heat history and pressure during CNT composite fabrication.[8] CNTs composed of C bonds are influenced by the existence of transition metals such as Fe and Ni at high temperature. The SPS sintering method is used for solidification sintering at low temperature and required only a short time in this research.

Figure 5 shows the relation between the sintering temperature and relative density of the SPS sintered body of Ni and the Ni/1 vol%CNT composite. In sintering Ni, at an increased densification temperature of up to 1073 K, the relative density also increases. When the sintering condition is similarly investigated with 1 vol%CNT composite, exactly the same result is observed at 1073 K.

The 2–10 vol%CNT composite is similarly sintered according to this condition, as shown in Fig. 6. For the 10 vol%CNT composite, the relative density is slightly lower as compared to that of the 0–5 vol%CNT composite, while the 0–5 vol%CNT composite is almost fully densified at 1073 K. The cause for low density of the 10 vol%CNT composite is thought to be the effect of the sintering obstruction by the CNT. This action becomes significant in the 10 vol%CNT composite because the increased amount of CNT does not inhibit the increased densification.

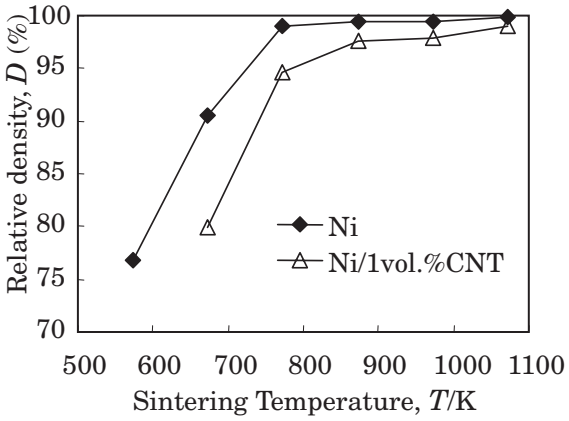

Fig. 5 Relative density of sintered body as a function of sintering temperature.

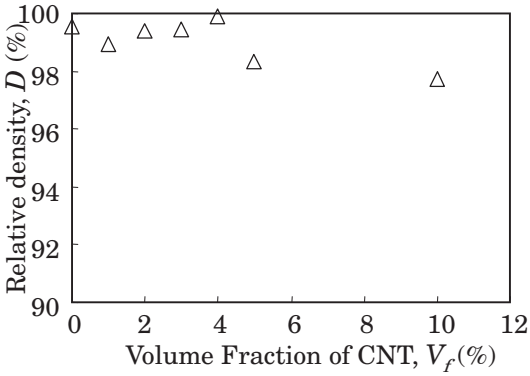

Fig. 6 Relative density of sintered body as a function of CNT volume content.

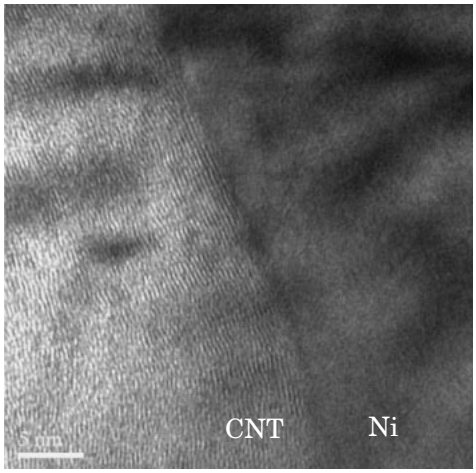

Fig. 7 TEM images of the nanocomposites showing stuck boundary of carbon nanotubes in the matrix.

The microstructure of the Ni/CNT boundary is observed with a transmission electron microscope. Figure 7 shows that the lattice pattern of the CNT and Ni in the crystal structure is excellent at the interface. Moreover, there is no gap in the interface: the CNT and matrix have been joined.

Figures 8 and 9 show SEM images of the cross-sections of the composites. These sections were obtained after electrol-

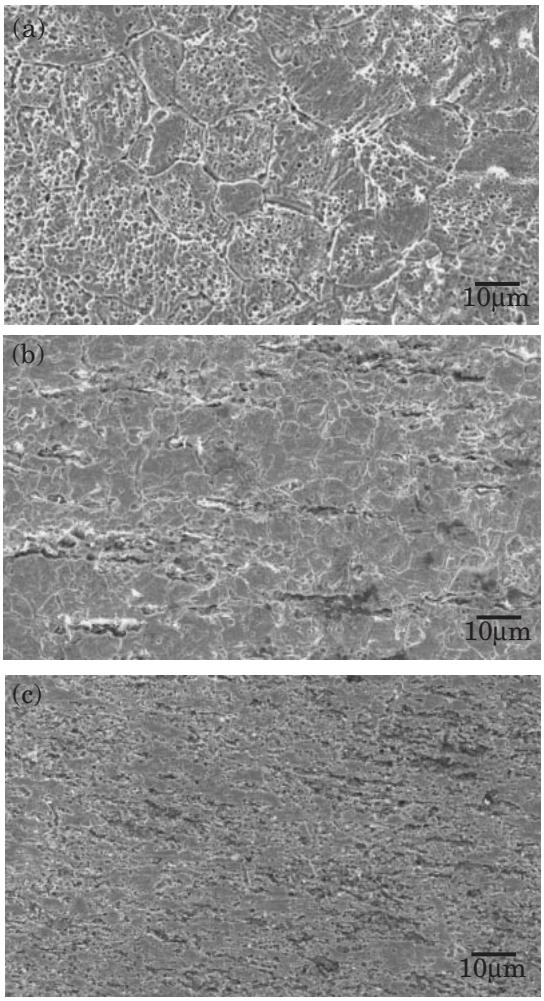

Fig. 8 Cross sectional area along the uniaxial compression (XZ plane) of sintering with (a) Ni100%, (b) Ni/1 vol%CNT and (c) Ni/5 vol%CNT at 1073 K.

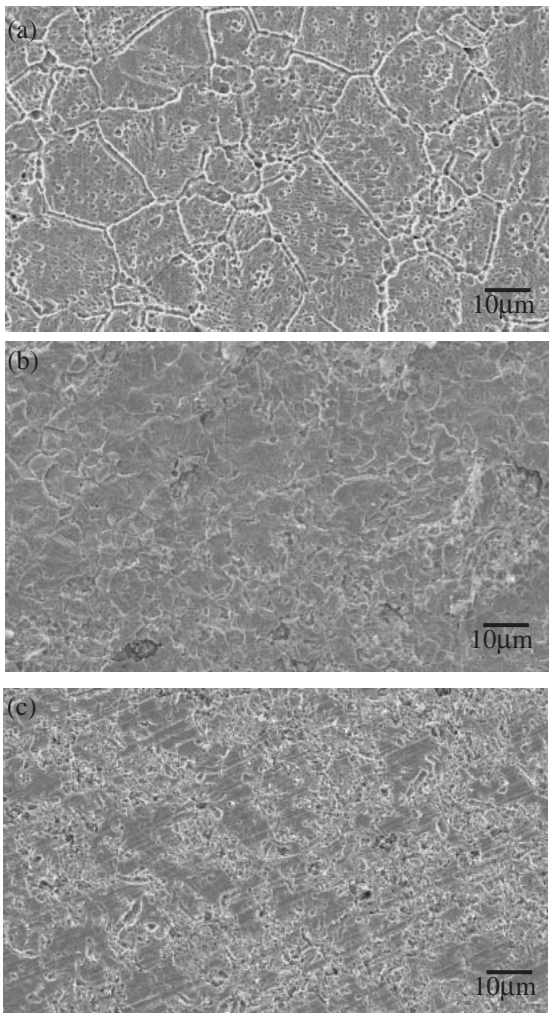

Fig. 9 Cross sectional area perpendicular to the pressing direction (XY plane) of sintering with (a) Ni100%, (b) Ni/1 vol%CNT and (c) Ni/5 vol%CNT at 1073 K.

ysis corrosion processing. The majority of the CNT exists in between the Ni particles. Moreover, as seen in the photograph for the Ni/1 vol%CNT composite, the CNT is concentrated only in certain parts. This concentration of CNT is observed to a lesser extent in the Ni/5 vol%CNT composite. The cause for the degradation of the dispersion of the CNT as compared to that of the dry body is considered as follows: (a) Densification occurs due to the growth during sintering. (b) The exhaust from Ni particles of CNT occurs because of the movement of Ni particles during densification, and the maintained uniform dispersion is lost in the precursor state. (c) On the other hand, the effect of the obstruction of grain growth strengthens the 5 vol% composite, which has a significant CNT content. It seems that the movement of CNT is decreased in the 5 vol% composite due to the driving power of the exhaust of CNT growth on Ni particles. The presence of bundled CNTs, as in Fig. 10, is confirmed in the CNT-concentrated parts of the sample. It is thought that the concentration of the CNT is emphasized because during sintering the low corrosion around the CNT neighborhood is less prioritized.

Composite structures have anisotropy in uniaxial pressure (perpendicular direction to photographs) during sintering.

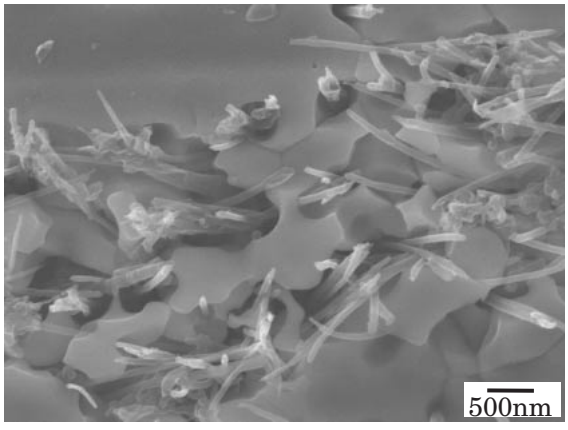

Fig. 10 CNT bundles of Ni/5 vol%CNT composite.

Figure 8 shows that a CNT is oriented perpendicularly to the pressing direction (Z direction) of the sintered composite body. The CNT is hardly observed in the perpendicular plane (XY plane) along the pressing direction. This is because CNTs orient parallel to the XY plane. The grain sizes of the composite become smaller than those of Ni100% because of

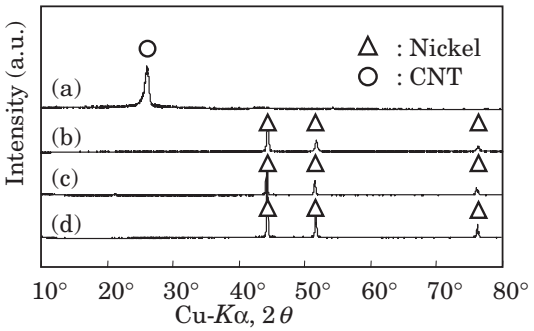

Fig. 11 XRD patterns of (a) CNT (b) raw nickel powder (c) sintered body of nickel and (d) Ni/10 vol%CNT after SPS.

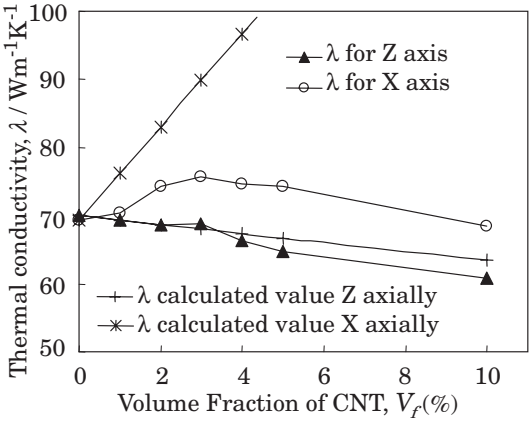

Fig. 12 Thermal conductivity as a function of CNT volume content.

the effect of sintering obstruction due to the existence of CNTs in between Ni particles. The characteristics of the CNT composites have been evaluated in relation to the influence of the grain size on the hardness and thermal conductivity of the material. The grain sizes of Ni100% and the 1 vol%CNT composite are approximately 12 µm and 5.3 µm in the cross-sectional area along the uniaxial compression direction (XZ plane), respectively. Moreover, the 5 vol%CNT composite is composed of very fine particles, and it is difficult to measure the accurate particle size along the XZ plane. The particle size is almost the same along the XZ and XY planes, which are perpendicular to the pressing direction. The 5 vol%CNT composite also has very fine grains along XY plane.

Figure 11 shows the XRD patterns for the raw Ni powder, raw CNT powder, sintered Ni100%, and sintered Ni/10 vol%CNT composites. Similar patterns were observed for raw powders and the sintered samples of the Ni100% and the Ni/10 vol%CNT composites and no new peaks appeared. It is thought that a new compound is not generated.

Moreover, when Ni100% is compared with the diffraction pattern of raw Ni powder, Ni powder is broader. The crystallinity of the raw Ni powder is lower than that of the sintered body. Crystallinity improves further for the raw Ni powder by the recovery and grain growth during sintering. It is thought that there is no influence on the CNT and Ni from the analysis results of XRD and the stability of Ni and carbon by sintering.

The observed anisotropy in Fig. 8 is grown in the structure of a sintered sample using SPS because the uniaxial pressure is applied during sintering. It is assumed that the thermal property is also similar. Figure 12 shows the thermal conductivity of each sintered sample at an SPS temperature of 1073 K. In addition to the experimental values, the calculated value of the thermal conductivity for each composition is calculated by the rule of mixtures. The thermal conductivity in the axial direction of the CNT is assumed to be 1500 W/mK[9,10] (approximately 900–1980 W/mK), the thermal conductivity in the cross-sectional (transverse) direction is assumed to be the thermal conductivity between graphene layers (5.5 W/mK).[11]

The thermal conductivity in the X direction was calculated using the expression below, considering the influence of the two-dimensional random distribution of the CNT. Moreover, the subsequent expression is used to easily calculate that in the pressing direction (Z direction).

$$\lambda_X = (1500/2 + 5.5/2) \times V_f/100 + \lambda_{Ni} \times (1 - V_f/100)$$
$$\lambda_Z = 5.5 \times V_f/100 + \lambda_{Ni} \times (1 - V_f/100) \quad (2)$$

Where V_f is content rate (vol%) and λ_{Ni} is the thermal conductivity (W/mK) of Ni. The thermal conductivity in the X direction increases as the CNT content increases up to 3 vol%. A slight increase in content is thought to be caused by a major effect so that the thermal conductivity of the CNT may considerably exceed the thermal conductivity of approximately 70 W/mK for Ni. In addition, when the thermal resistance is small on the Ni/CNT interface, the high-thermal conductivity of the CNT becomes effective in heat conduction within the composite.[12] It is expected that the thermal resistance at the interface shown in Fig. 7 is small.

The thermal conductivity in the X direction decreases at 4 vol% or greater. The thermal conductivity in the X direction almost decreases to the level of that of Ni at 10 vol%. It is thought that the CNT forms bundles when the CNT content increases because the thermal conductivity decreases by phonon-phonon scattering of CNT when CNT bundles are formed.[13] It seems that the thermal conductivity in the X direction decreased because the ratio with which CNT forms bundles increases with the CNT content rate.

The experimental values of the thermal conductivity are lower compared with the calculated values because there is a cause to which some thermal conductivities decrease besides the decrease in the thermal conductivity due to the formation of CNT bundles.[14] CNT winding is a phenomenon that inevitably occurs in composites fabricated by powdery metallurgy techniques, although there is a report that the thermal conductivity of CNT decreases when the CNT winds. Because the specific surface area is large, the interfacial influence of the minute CNTs on the heat conduction is also very large. Thus, it is necessary to consider the thermal resistance at the interfaces for this effect. An effective result was not obtained, although research on the improvement of thermal conductivity by combining CNTs has been conducted as stated above. However, the increase in thermal conductivity due to the content of CNT shows the possibility of the application of metallic materials to improve the thermal conductivity of CNTs.

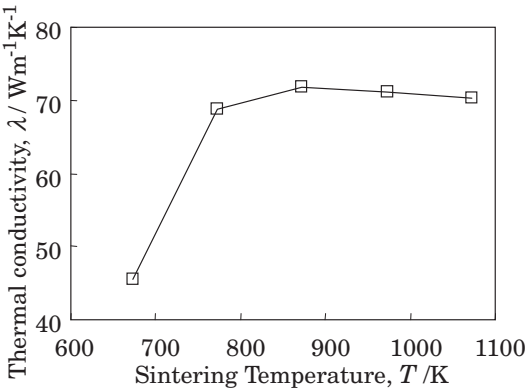

Fig. 13 Thermal conductivity of Ni/1 vol%CNT as a function of sintering temperature.

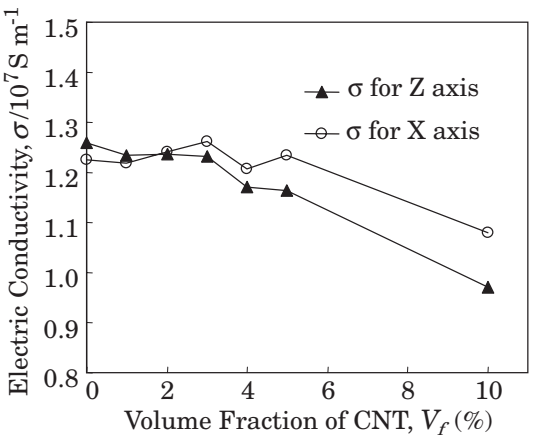

Fig. 14 Electrical conductivity as a function of CNT volume content.

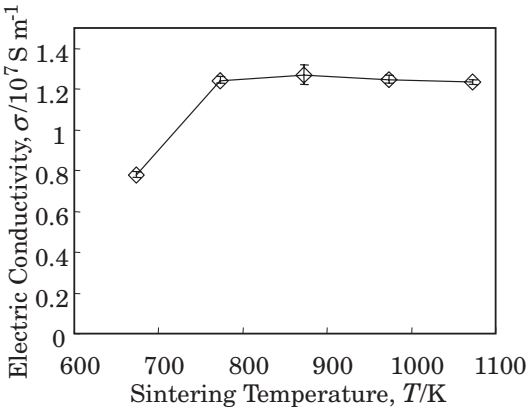

Fig. 15 Electrical conductivity of Ni/1 vol%CNT as a function of sintering temperature.

The thermal conductivity in the pressing direction (Z direction) decreased as the CNT content increased (Fig. 12). The thermal conductivity of the CNT oriented in the X direction is more appreciable. It is expected that the CNT has a higher thermal conductivity along the transverse direction than along the radial axis.[13] Therefore, it is presumed that the thermal conductivity of the composite decreases with an increase in the CNT volume content.

In the same manner as the other causes an increase in the grain boundary due to a decrease in grain size reduces the thermal conductivity. The thermal conductivity decreases along the grain boundary, generating resistance to the flow of heat. The grain size of the sintered CNT composite becomes small as compared to that of Ni100% due to the grain-growth controlling effect in the CNT composite; the resistance of the grain boundary may also increase. In addition, it is necessary to consider the decrease in the thermal conductivity due to the decrease in density in the 10 vol% sample.

The thermal conductivity of the Ni/1 vol%CNT composite sintered at 673–1073 K by SPS sintering along the X direction is shown in Fig. 13. The thermal conductivity increases with the sintering temperature, and the highest thermal conductivity is obtained at 873 K. When the sintering temperature is 973 K and 1073 K, the thermal conductivity decreases below that at 873 K. The reasons for the rise in thermal conductivity at 873 K as the sintering temperature rises are sought. An increase in the relative density and the recovery of Ni may occur. In addition, it is possible that the thermal resistance at the grain boundary decreases so that the grain boundary may decrease with grain growth. The samples sintered at 973 K and 1073 K were investigated and compared with the samples sintered at 873 K and the following is thought to be the reason why the thermal conductivity decreases slightly. When the movement of CNTs is caused by the Ni-particle growth as sintering progresses, the decentralization of the CNTs is destroyed and the CNTs form bundles. It is thought that the thermal conductivity decreases because of the considerable movement of CNTs that occurs as it is sintered at high temperature, and the CNT bundling intensifies. The particle size increases as the sintering progresses at a high temperature and the density rises. This phenomenon does not seem to relate to a remarkable decrease in thermal conductivity because the rising effect of the thermal conductivity on the density increase is counterbalanced by the decrease in the thermal conductivity due to bundle formation.

The electrical conductivity perpendicular to the pressing direction (X direction) is shown in Fig. 14. The electrical conductivity shows almost a constant value up to a CNT content of 5 vol% and decreases thereafter. The electrical conductivity of CNT is reported to be approximately $1–2 \times 10^5$ S m^{-1}[15] and that for the Ni matrix is 100–1000 times this value. The expected value prior to experiment seemed that the electrical conductivity of CNT used in this research shows a promising value compared to the previous published values.

The electrical conductivity along the pressing direction (Z direction) decreases as the CNT content rate increases. It is expected that the high electric conductivity as well as the thermal conductivity of the CNT is only axially demonstrated. This shows that the electrical conduction along the X direction (CNT oriented direction) is higher than that along a direction perpendicular to the pressing direction (Z direction).

Figure 15 shows the electrical conductivity of the Ni/1 vol%CNT composite sintered at 673–1073 K. The electrical conductivity increases with the sintering temperature, and the highest electrical conductivity is obtained at 873 K. When the sintering temperature is 973 K, the electrical conductivity decreases as compared to that at 873 K, and it decreases

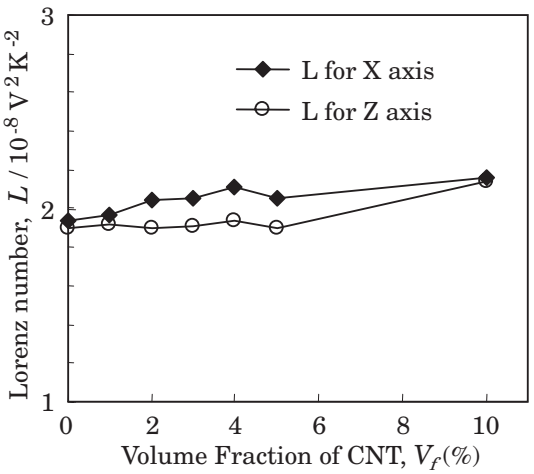

Fig. 16 Lorenz number calculated measurements as a function of CNT volume content.

further at 1073 K. This agrees well with the influence of the sintering temperature on the thermal conductivity.

Figure 16 shows the relation between the Lorentz number calculated from the experimental values of the thermal and electrical conductivities and the CNT content. The Lorentz number shows a slight increase as the CNT content rate increases. It is thought that the electron contribution from the CNT is small, although heat conduction of Ni, which is a metal, happens predominantly by electron conduction. With CNT, it is considered that the Lorentz number is approximately $L = \lambda/(\sigma T) = 5 \times 10^{-6}\,V^2/K^2$ (based on the thermal and electrical conductivities of a single-walled CNT mat) at room temperature, and the contribution from the conduction electrons is small because this value is just larger than $L_0 = 2.45 \times 10^{-8}\,V^2/K^2$, as calculated from the Wiedermann-Franz rules.[16] However, the Lorentz number for each composition shows that the contribution to heat conduction due to electron conduction cannot be disregarded even at room temperature (298 K). Recently, the possibility of electrical conduction in singlewall nanotubes, which is ballistic conduction, has been theoretically shown,[17] that is, it has been theoretically predicted that ballistic conduction occurs without resistance due to the disappearance of backscattering. When scattering occurs during electric conduction very few ballistics are produced;[18–20] thus, the contribution of free electrons to heat conduction is due to the multiwall nanotube. This problem will be tackled in future reports, although explicit consideration becomes possible only by obtaining the temperature dependencies of the Lorentz number.

4. Conclusion

This research focused on CNT and metal matrix composites. Ni fine powder was selected as the metal to be combined with the CNT. A homogeneous colloid mixing process was adopted, and the SPS method was used for fabricating the Ni/CNT composite and to distribute and combine the MWNT in the Ni. The influence of the sintering conditions on the sintered body was examined, including the influence of the CNT content and the process conditions on the structure and the characteristics of the Ni/CNT composite. The following conclusions were obtained:

(1) The Ni/CNT composite was fabricated using SPS method to solidify and sinter in a short time. The sintered body revealed that there was no gap between the interface and CNT.

(2) For a CNT content of 3 vol%, the thermal conductivity along the SPS pressing direction increased with the CNT content. A small increase in the content is thought to have a large effect on the thermal conductivity of the CNT, which may greatly exceed the thermal conductivity of approximately 70 W/mK for Ni. The thermal conductivity decreases when the CNT content increases beyond 4 vol%, and the thermal conductivity decreases to this level of that of Ni100% at 10 vol%. The decrease in thermal conductivity is thought to be caused by CNT bundle formation.

(3) The electrical conductivity of the 5 vol%CNT shows an almost constant value, and the electrical conductivity decreases along the SPS pressing direction as compared to that perpendicular to the pressing direction. This is explained by the electrical conduction due to the ballistic effect reported for multilayer nanotubes.

(4) It is shown that the contribution to the heat of conduction from the conduction electrons due to the change in the Lorentz number should not be disregarded for measurements at room temperature (298 K). The multilayer nanotubes cause very little scattering during electrical conduction.

REFERENCES

1) S. Iijima: Nature **354** (1991) 56–58.
2) Y. S. Song and J. R. Youn: Carbon **44** (2006) 710–717.
3) M. B. Bryning, D. E. Milkie, M. F. Islam, J. M. Kikkawa and A. G. Yodh: Appl. Phys. Lett. **87** (2005) 161909.
4) S. Song and J. R. Youn: Carbon **43** (2005) 1378–1385.
5) G. D. Zhan and A. K. Mukherjee: Int. J. Appl. Ceram. Technol. **1** (2004) 161–171.
6) R. Watanabe and Y. Masuda: J. Japan Inst. Metals **45** (1981) 781–789.
7) C. R. Barrett, W. D. Nix and A. S. Tetelman: *Zairyoukagaku1* (Baifuudou, 1979) pp. 200–201.
8) E. Flahaut, A. Peigney, Ch. Laurent, Ch. Marlie, F. Chastel and A. Rousset: Acta Mater. **48** (2000) 3803–3812.
9) P. Kim, L. Shi, A. Majumdar and P. L. McEuen: Phys. Rev. Lett. **87** (2001) 215502.
10) S. Berber, Y. K. Kwon and D. Tomanek: Phys. Rev. Lett. **84** (2000) 4613–4616.
11) J. Che, T. Cagin and W. A. Goddard: Nanotechnology **11** (2000) 65–69.
12) C. W. Nan, Z. Shi and Y. Lin: Chem. Phys. Lett. **375** (2003) 666–669.
13) J. Hone, M. C. Llaguno, N. M. Nemes, A. T. Johnson, J. E. Fischer, D. A. Walters, M. J. Casavant, J. Schmidt and R. E. Smalley: Appl. Phys. Lett. **77** (2000) 666–668.
14) H. Stahl, J. Appenzeller, R. Martel, Ph. Avouris and B. Lengeler: Phys. Rev. Lett. **85** (2000) 5186–5189.
15) K. Kaneto, K. Tsuruta, M. Sakai, W. Y. Cho and Y. Ando: Synthetic Met. **103** (1999) 2543–2546.
16) J. Hone, M. Whitney, C. Piskoti and A. Zettl: Phys. Rev. B **59** (1999) 2514–2516.
17) L. Chico, L. X. Mendic, S. G. Louie and M. L. Cohen: Phys. Rev. B **54** (1996) 2600.
18) A. Kanda and K. Tsukagoshi: Parity **18** (2003) 36–40.
19) S. Frank, P. Poncharal, Z. L. Wang and W. A. de Heer: Science **280** (1998) 1744.
20) A. Urbina, I. Echeverria and J. Abellan: Phys. Rev. Lett. **90** (2003) 106603.